PHYSICAL REVIEW LETTERS

Analytic Gravitational Waveforms for Generic Precessing Binary Inspirals

Katerina Chatziioannou,[1] Antoine Klein,[2,3] Neil Cornish,[1] and Nicolás Yunes[1]

[1]*eXtreme Gravity Institute, Department of Physics, Montana State University, Bozeman, Montana 59717, USA*
[2]*Department of Physics and Astronomy, The University of Mississippi, University, Mississippi 38677, USA*
[3]*CENTRA, Departamento de Física, Instituto Superior Técnico, Universidade de Lisboa,*
Avenida Rovisco Pais 1, 1049 Lisboa, Portugal

Binary systems of two compact objects circularize and spiral toward each other via the emission of gravitational waves. The coupling of the spins of each object with the orbital angular momentum causes the orbital plane to precess, which leads to modulation of the gravitational wave signal. Until now, generating frequency-domain waveforms for fully precessing systems for use in gravitational wave data analysis meant numerically integrating the equations of motion, then Fourier transforming the result, which is very computationally intensive for systems that complete hundreds or thousands of cycles in the sensitive band of a detector. Previously, analytic solutions were only available for certain special cases or for simplified models. Here we describe the construction of closed-form, frequency-domain waveforms for fully precessing, quasicircular binary inspirals.

The recent detection of gravitational waves from a binary black hole merger by LIGO [1], with a signal that is in accordance with the predictions of Einstein's theory [2–4], is a triumph of engineering and theoretical physics. The GW150914 signal provided our first observational encounter with strong field, dynamical gravity, as well as a chance to compare predictions with data. Efforts to model the orbital evolution of such binary systems and their gravitational wave emission have been ongoing for a century [5]. The nonlinearity of Einstein's field equations greatly complicates the solution to the gravitational two-body problem, with the fixed elliptical orbits of Newton's theory replaced by orbits that tilt and precess as the bodies spiral inward and eventually merge.

While complete solutions to the two-body problem in general relativity are only known numerically, accurate approximations are available for describing the early inspiral where the orbital velocity v is small compared to the speed of light. These post-Newtonian (PN) equations of motion are known completely to $\mathcal{O}(v^6)$ and partially to $\mathcal{O}(v^7)$ [5]. The effective-one-body (EOB) formalism [6], along with calibration against solutions from numerical relativity [7–12], have been able to extend the analytic description through merger and ringdown for binary black holes. Solving the PN equations of motion analytically is challenging, especially when the orbits are eccentric or the bodies are spinning. While solving the PN equations numerically is far less intensive than solving the full Einstein equations, it can add days or weeks to Bayesian parameter estimation studies [13,14]. Moreover, since most analyses are performed in the frequency domain, we seek closed-form solutions that can be computed directly in frequency. For non-recessing systems, this can be done

using the stationary phase approximation, but this approximation fails for precessing systems.

Closed-form, analytic waveform models for spin-precessing systems currently exist for several special cases. The first are for systems where only one object is spinning [15]. The ensuing motion is simple precession, and the resulting waveform is ideal for black-hole–neutron-star (BHNS) systems [16]. Related to these are waveforms described by effective spin parameters that provide good matches to fully precessing waveforms [17]. The effective spin approach has been used to produce approximate analytic waveforms describing the full inspiral, merger, and ringdown of spinning black hole binaries [18,19]. Analytic solutions have also been found for nearly aligned [20] and slowly spinning [21] systems. The latter are accurate representations of neutron-star–neutron-star (NSNS) inspirals, both for detection and parameter estimation [22–24].

Here we describe the construction of accurate, closed-form, frequency-domain waveforms for fully precessing, quasicircular PN inspirals. The solution utilizes three main elements: the recently discovered reduction to quadratures for the conservative precessional dynamics [25], multiple scale analysis (MSA) to exploit the natural separation of time scales of the PN dynamics, and the shifted uniform asymptotic (SUA) method for performing Fourier transforms of waveforms with caustics [26]. For most systems, the waveforms accurately match those found by numerically evolving the equations of motion and Fourier transforming the gravitational wave signal. The minority that fail can be caught in advance and computed numerically.

The PN expansion naturally introduces a separation of time scales: Newtonian dynamics at $\mathcal{O}(v^0)$, the first

relativistic effects such as periastron precession at $\mathcal{O}(v^2)$, spin-orbit coupling at $\mathcal{O}(v^3)$, spin-spin coupling at $\mathcal{O}(v^4)$, orbital decay at order $\mathcal{O}(v^5)$, and so on. Ignoring dissipation, the precession equations for circular orbits can be orbit averaged to yield a closed set of nine coupled, first-order ordinary differential equations for the spin angular momenta of the two bodies $\boldsymbol{S}_1$, $\boldsymbol{S}_2$ and the orbital angular momentum $\boldsymbol{L}$. These equations admit seven conserved quantities, $\{S_1, S_2, L, J, \xi\}$, where $\boldsymbol{J} = \boldsymbol{L} + \boldsymbol{S}_1 + \boldsymbol{S}_2$ is the total angular momentum; S_1, S_2, and L are the magnitudes of the angular momenta three-vectors; and ξ is the mass-weighted effective spin

$$\xi \equiv (1 + q)\boldsymbol{S}_1 \cdot \hat{\boldsymbol{L}} + (1 + q^{-1})\boldsymbol{S}_2 \cdot \hat{\boldsymbol{L}}, \qquad (1)$$

where $q = m_2/m_1$ is the mass ratio. Kesden *et al.* [25] showed that by working in a noninertial, co-precessing frame of reference, the motion could be reduced to quadratures in terms of the squared spin magnitude $S^2 = (\boldsymbol{S}_1 + \boldsymbol{S}_2)^2$:

$$\left(\frac{dS^2}{dt}\right)^2 = -A^2(S^6 + BS^4 + CS^2 + D), \qquad (2)$$

where the constants $\{A, B, C, D\}$ are given in terms of the seven conserved quantities. Rather than integrate this equation numerically [25], we were able to find a closed-form solution in terms of Jacobi elliptic functions:

$$S^2 = S_+^2 + (S_-^2 - S_+^2)\mathrm{sn}^2(\psi, m), \qquad (3)$$

where sn is the sinelike Jacobi elliptic function with modulus $m = (S_+^2 - S_-^2)/(S_+^2 - S_3^2)$ and phase $\psi = (A/2)\sqrt{S_+^2 - S_3^2}\, t$, where $\{S_+^2, S_-^2, S_3^2\}$ are the roots of the cubic that appears on the right-hand side of Eq. (2). The solution is completed by solving for the precession angle ϕ_z between $\boldsymbol{L}_\perp = \boldsymbol{L} - (\hat{\boldsymbol{J}} \cdot \boldsymbol{L})\hat{\boldsymbol{J}}$ and the $\hat{\boldsymbol{x}}$ direction in a coordinate system where $\hat{\boldsymbol{J}}$ defines the $\hat{z}$ direction and $\boldsymbol{L}_\perp$ at some reference frequency defines the $\hat{\boldsymbol{x}}$ direction. The rate of precession $\Omega_z = \dot{\phi}_z$ is given by

$$\frac{\Omega_z}{J} = a + \frac{c_0 + c_2\mathrm{sn}^2(\psi, m) + c_4\mathrm{sn}^4(\psi, m)}{d_0 + d_2\mathrm{sn}^2(\psi, m) + d_4\mathrm{sn}^4(\psi, m)}, \qquad (4)$$

where the constants $\{a, c_0, c_2, c_4, d_0, d_2, d_4\}$ are given in terms of the seven constants of motion and the orbital velocity. This equation can be integrated to give ϕ_z in terms of elliptic integrals. The remaining angles needed to specify $\boldsymbol{S}_1$, $\boldsymbol{S}_2$, and $\boldsymbol{L}$ are given in terms of $S(t)$ and the constants of motion. This completes the construction of a closed-form, analytic solution to the conservative dynamics.

The emission of gravitational radiation causes the system to lose energy and angular momentum. Here we can use the separation between the precession time scale $T_{\mathrm{pr}} \equiv |\boldsymbol{S}_1|/|\dot{\boldsymbol{S}}_1| \sim v^{-5}$ and the radiation-reaction time scale $T_{\mathrm{rr}} \equiv v/\dot{v} \sim v^{-8}$ to develop a MSA solution that incorporates

dissipation. For most variables, we find that the leading-order term in the MSA is sufficient. Additional accuracy could be achieved by continuing to higher order in the expansion. Of the original seven constants of motion, the spin magnitudes $\{S_1, S_2, \xi\}$ remain constant under radiation reaction. While the magnitude of the total angular momentum J changes as L decays, the direction $\hat{\boldsymbol{J}}$ remains almost constant. This can be established by precession averaging and PN expanding the evolution equation $\dot{\hat{\boldsymbol{J}}} = \dot{L}\hat{\boldsymbol{L}}/J - \dot{J}\hat{\boldsymbol{J}}/L$ to show that $\hat{\boldsymbol{J}}_z$ is constant to $\mathcal{O}(v^2)$, while $\hat{\boldsymbol{J}}_{x,y}$ oscillate but exhibit no secular growth at $\mathcal{O}(v^2)$. Since the wobble in $\hat{\boldsymbol{J}}$ is very small, we are able to neglect this variation and continue to use $\hat{\boldsymbol{J}}$ to define our coordinate system. This preserves the geometrical framework used to solve the spin-precession equations.

The orbital angular momentum depends on the orbital velocity as $L = (m_1 + m_2)\eta/v$, where $\eta = m_1 m_2/(m_1 + m_2)^2$ is the symmetric mass ratio. Precession averaging and PN expanding the evolution equation for J yields $J^2 = L^2 + 2c_1/v + c_2 + \mathcal{O}(v)$, where c_1 and c_2 are constants that are set by the initial conditions at some reference frequency. The evolution of L and J causes the roots $\{S_+^2, S_-^2, S_3^2\}$ to evolve on the radiation-reaction time scale: $S_\pm^2 = S_{\pm,0}^2 + \mathcal{O}(v)$ and $S_3^2 = \mathcal{O}(v^{-2})$. The MSA solution for S^2 follows from adiabatically promoting the constants in Eq. (3) to functions of time. To leading order, the amplitudes of the oscillations in S^2 are constant, while the modulus grows as $m \sim v^2$; thus, the oscillations become increasingly anharmonic as the masses spiral towards each other. The phase ψ can be PN expanded and integrated: $\psi = \psi_0 - 3g_0(m_1 - m_2)(1 + \psi_1 v + \psi_2 v^2 + \ldots)/(4v^3)$, where $\{\psi_0, g_0, \psi_1, \psi_2\}$ are constants that depend on the masses, spins, and initial conditions. Comparison with the numerical solution shows that the leading-order MSA solution for S^2 is very accurate, so there is no need to continue to higher orders in the expansion. Finding a solution for ϕ_z to complete the derivation for precessional motion with dissipation turns out to be the most challenging step. To compute the MSA, we introduce two time variables, the precession time t_{pr} and the radiation-reaction time t_{rr}. The leading-order term in the MSA is found by precession averaging Ω_z and PN integrating:

$$\phi_{z,-1} = \int \langle\Omega_z\rangle_{\mathrm{pr}}(t_{\mathrm{rr}})dt_{\mathrm{rr}} = \int \langle\Omega_z\rangle_{\mathrm{pr}}\frac{dv}{\dot{v}}. \qquad (5)$$

While this leading-order term captures the overall secular evolution of ϕ_z, we found that the agreement between the numerical and analytic solutions could be improved by including the second-order term in the MSA expansion,

$$\phi_{z,0} = \int \Omega_z(t_{\mathrm{pr}}, t_{\mathrm{rr}})dt_{\mathrm{pr}} - \int \langle\Omega_z\rangle_{\mathrm{pr}}(t_{\mathrm{rr}})dt_{\mathrm{pr}}, \qquad (6)$$

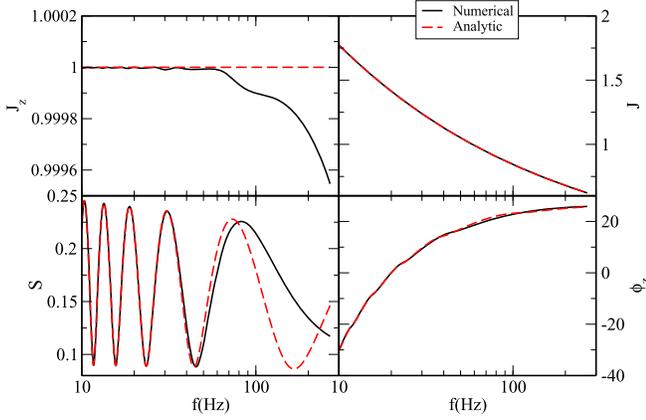which describes small oscillations in ϕ_z on the precession time scale.

FIG. 1.   A comparison of the analytic (red dashed lines) and numerical (black solid lines) solutions to the PN equations of motion for a strongly precessing black hole binary. Clockwise from the upper left, we have the frame orientation $\hat{J}_z$, the magnitude of the total angular momentum J, the precession angle ϕ_z, and the magnitude of the total spin S. The largest discrepancy between the solutions occurs for S and can be traced to the approximate phasing ψ. However, as shown in Fig. 2, the impact on the waveform is minor.

Figure 1 compares the analytic and numerical solutions for $\hat{J}_z$, J, S, and ϕ_z for a strongly precessing black-hole–black-hole (BHBH) binary with masses $(m_1, m_2) = (10, 7)M_\odot$ and spin magnitudes $(S_1, S_2) = (0.6m_1^2, 0.7m_2^2)$. The angles between the spins and angular momentum at a reference frequency of 20 Hz are $L, S = 78°$, $L, S_1 = 120°$, and $L, S_2 = 36°$. Overall, the agreement is excellent. The largest discrepancy occurs in the spin magnitude, and it is due to the difference between the numerical and analytic solutions for the phase ψ. It is possible to improve the agreement by continuing the PN expansion of ψ to higher order, but this is unnecessary since the dephasing in S has little impact on the waveforms. Note that the waveform was truncated at $r = 6(m_1 + m_2)$ and does not extend to cover the merger and ringdown portions of the full signal.

With the analytic solution for the orbital motion in hand, the next step is to produce the gravitational waveforms in the frequency domain using the SUA transform. The gravitational wave signal emitted by a binary system in general relativity as observed in an interferometric detector is $h(t) = F_+ h_+ + F_\times h_\times$, where $(F_+, F_\times)$ are the antenna pattern functions and $(h_+, h_\times)$ are the two polarization states of the gravitational wave signal. The polarization states for a source located in the $\hat{N}$ direction can be decomposed into a spin-weighted spherical harmonic basis [27]

$$h_+ - ih_\times = \sum_{l \geq 2} \sum_{m=-l}^{l} H_{lm}(\theta_s, \phi_s) e^{-im\Phi}, \quad (7)$$

where $\Phi = \phi_{\rm orb} - 3v^3(2 - \eta v^2) \ln v$, $\phi_{\rm orb}$ is the orbital phase, (θ_s, ϕ_s) are the spherical angles of $\hat{N}$ in a frame where $\hat{J}$ is along the z axis, and

$$H_{lm} = h^{lm} \sum_{m'=-l}^{l} D_{m',m}^l(\phi_z, \theta_L, \zeta)\,_{-2}Y_{lm'}(\theta_s, \phi_s), \quad (8)$$

where the amplitudes h^{lm} can be found in Ref. [5], $D_{m,m'}^l$ are the Wigner D matrices, $_sY_{lm}$ are the spin-weighted spherical harmonics, the angles θ_L and ϕ_z are the spherical angles of $\hat{L}$ in the same frame as θ_s and ϕ_s are defined, and ζ satisfies $\dot{\zeta} = \dot{\phi}_z \cos\theta_L$. In order to solve for ζ, we employ the same MSA techniques as for ϕ_z.

To compute the Fourier transform of h, we use the SUA method devised in Ref. [26] and write

$$\tilde{h}(f) = \sqrt{2\pi} \sum_{m \geq 1} T_m e^{i(2\pi f t_m - m\Phi - \pi/4)}$$

$$\times \sum_{l \geq 2} \sum_{k=-k_{\rm max}}^{k_{\rm max}} \frac{a_{k,k_{\rm max}}}{2 - \delta_{k,0}} \mathcal{H}_{lm}(t_m + kT_m), \quad (9)$$

where t_m and T_m are defined implicitly by $2\pi f = m\dot{\Phi}(t_m)$, $T_m = (m\ddot{\Phi}(t_m))^{-1/2}$, and

$$\mathcal{H}_{lm} = \frac{1}{2}(F_+ + iF_\times)H_{lm} + \frac{1}{2}(F_+ - iF_\times)H_{l,-m}, \quad (10)$$

with the constants $a_{k,k_{\rm max}}$ satisfying the linear system

$$\frac{(-i)^p}{2^p p!} = \sum_{k=0}^{k_{\rm max}} a_{k,k_{\rm max}} \frac{k^{2p}}{(2p)!}, \quad (11)$$

for $p \in \{0, ..., k_{\rm max}\}$. For a static detector, $\mathcal{H}_{lm}$ depends on frequency only through ϕ_z, θ_L, and ζ. As shown in Ref. [26], setting $k_{\rm max} = 3$ is sufficient to accurately match the numerical Fourier transform.

Figure 2 compares the numerical and analytic solutions for the amplitude and phase of the gravitational waveform h produced by the system shown in Fig. 1, observed edge-on and located on the detector plane at the initial reference time. There is good agreement across the band, with the dephasing at high frequencies coming from errors in the PN integrated phase ψ. The discrepancy has little effect on the overlap between the waveforms, which we measure in terms of the faithfulness, defined as

$$F \equiv \max_{t_c, \phi_c} \frac{(h_1|h_2)}{\sqrt{(h_1|h_1)(h_2|h_2)}}, \quad (12)$$

where t_c and ϕ_c are the merger time and phase, and $(a|b)$ denotes the usual noise-weighted inner product. Using the aLIGO design zero-detuning, high-power noise spectral density [28], the faithfulness of the analytic waveform shown in Fig. 2 is $F = 0.9997$.

We tested the analytic waveforms for a wider range of signals through a Monte Carlo study that covered NSNS,
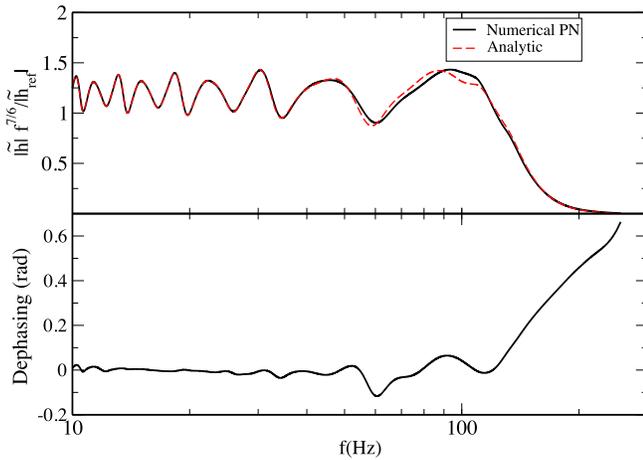
FIG. 2.   A comparison of the analytic and numerical solutions for the Fourier amplitude (upper panel) and Fourier phase (lower panel) of the observed gravitational wave signal for a strongly precessing black hole binary. The amplitudes are scaled by a reference amplitude at 20 Hz, $|\tilde{h}_{\rm ref}| \equiv (20\ {\rm Hz})^{7/6}|\tilde{h}(f=20)|$, and multiplied by $f^{7/6}$ to account for the dominant secular evolution.
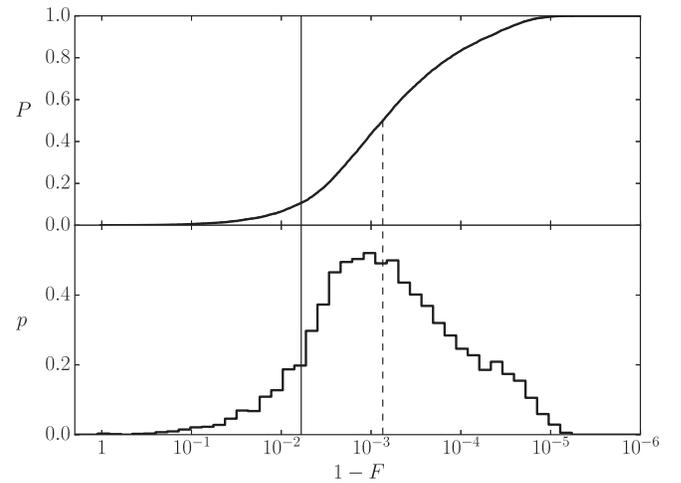

FIG. 3.   Cumulative (upper panel) and fractional (lower panel) distribution of the unfaithfulness, $1-F$, of the analytic waveforms for a sample of 10 000 precessing binary black hole systems. While the agreement between the numerical and analytic PN waveforms is excellent for the majority of systems, there exists a small subset that produce unacceptably high mismatches above a nominal threshold of $F = 0.994$ indicated by the solid vertical line. The dashed vertical line marks the median unfaithfulness, which corresponds to $1-F = 7.4 \times 10^{-4}$.

NSBH, and BHBH binaries. Here we focus on the BHBH systems since they have the most complicated precessional dynamics, and their inspiral is not described by existing analytic methods. The Monte Carlo study drew 10,000 systems with masses drawn uniformly in logarithm between $[2.5, 20]M_\odot$, and dimensionless spin magnitudes S_i/m_i^2 drawn uniformly in [0, 1]. The initial directions of the unit vectors $\{\hat{L}, \hat{S}_1, \hat{S}_2\}$ and the sky location $\hat{N}$ were drawn randomly on the sphere. Figure 3 shows the distribution of the unfaithfulness $1-F$ for this sample. We demand that the systematic errors introduced by waveform modeling errors are smaller than the statistical errors. This requires choosing a reference SNR for the systems of interest, as the statistical errors scale with the SNR while the systematic errors are SNR independent [29]. It can be shown that the expected value for the faithfulness due to statistical errors in the intrinsic parameters is given by $F = 1 - D_{\rm in}/(2{\rm SNR}^2)$, where $D_{\rm in}$ are the number of intrinsic parameters. Choosing a reference SNR = 25 and using that $D_{\rm in} = 8$, we obtain a nominal accuracy threshold of $F = 0.994$. We found that 10.7% of BHBH systems fell outside of this accuracy requirement (for NSNS binaries, the fraction was 0.3%, and for BHNS binaries 1.6%). We found that systems with very low overlaps $F < 0.97$ fell into three categories. The first category includes systems with total angular momenta J and orbital angular momenta L that pass through near-anti-alignment during the evolution of the orbit, which leads to a problem with our coordinate system which is defined by $J = L + S$ and $L \times J$. In particular, the ϕ_z coordinate becomes ill defined when S and L are parallel. So long as the alignment is not perfect, the numerical solution proceeds smoothly, while

the analytic MSA PN expansion of ϕ_z has coefficients in the velocity expansion that diverge. The second category of troublesome cases are nearly edge-on systems, $(L \cdot N \sim 0)$, a configuration which maximizes the effects of precession on the waveforms and amplifies any small inaccuracies in the analytic solution. The third category of bad systems were found to undergo transitional precession [15]. We found that the overlaps could be improved in all cases by going to higher order in the MSA and the PN integration, but to fully solve the problem, one will likely need a change of coordinates. In data analysis applications, the troublesome systems can be caught in advance and other, slower methods, such as the numerical SUA [26], can be used to generate the waveforms. By a change of coordinates, or by some other means, it should be possible to modify the ϕ_z solution so that it can handle spin-orbit anti-alignment and transitional precession. Extending the analytic solution to higher order will improve the fitting factor for edge-on systems. We leave these extensions to future work.

In summary, we have described the derivation of the first closed-form, frequency-domain waveforms for fully precessing compact binary inspiral. Complete details will be provided in a longer follow-up paper. The method described here can be extended to cover the full inspiral, merger, and ringdown stages of a black hole merger using EOB or phenomenological waveforms. In particular, our work allows for the development of fully precessing variants of the effective-spin "PhenomP" waveforms [18,19]. The new waveforms are typically much faster to compute than traditional numerical, time-domain implementations—up to 3

orders of magnitude faster for NS-NS binaries starting from 10 Hz. The analytic solution also provides additional physical insight into the dynamics.

---

[1] B. P. Abbott *et al.* (Virgo and LIGO Scientific Collaborations), Phys. Rev. Lett. **116**, 061102 (2016).

[2] B. P. Abbott *et al.* (Virgo and LIGO Scientific Collaborations), Phys. Rev. Lett. **116**, 221101 (2016).

[3] N. Yunes, K. Yagi, and F. Pretorius, Phys. Rev. D **94**, 084002 (2016).

[4] B. P. Abbott *et al.* (Virgo and LIGO Scientific Collaborations), Phys. Rev. D **94**, 064035 (2016).

[5] L. Blanchet, Living Rev. Relativ. **17**, 2 (2014).

[6] A. Buonanno and T. Damour, Phys. Rev. D **59**, 084006 (1999).

[7] A. Buonanno, Y. Pan, H. P. Pfeiffer, M. A. Scheel, L. T. Buchman, and L. E. Kidder, Phys. Rev. D **79**, 124028 (2009).

[8] P. Ajith *et al.*, Phys. Rev. Lett. **106**, 241101 (2011).

[9] Y. Pan, A. Buonanno, A. Taracchini, L. E. Kidder, A. H. Mrou, H. P. Pfeiffer, M. A. Scheel, and B. Szilgyi, Phys. Rev. D **89**, 084006 (2014).

[10] A. Taracchini *et al.*, Phys. Rev. D **89**, 061502 (2014).

[11] L. Santamaría *et al.*, Phys. Rev. D **82**, 064016 (2010).

[12] S. Khan, S. Husa, M. Hannam, F. Ohme, M. Pürrer, X. J. Forteza, and A. Bohé, Phys. Rev. D **93**, 044007 (2016).

[13] J. Veitch *et al.*, Phys. Rev. D **91**, 042003 (2015).

[14] B. Farr *et al.*, Astrophys. J. **825**, 116 (2016).

[15] T. A. Apostolatos, C. Cutler, G. J. Sussman, and K. S. Thorne, Phys. Rev. D **49**, 6274 (1994).

[16] A. Lundgren and R. O'Shaughnessy, Phys. Rev. D **89**, 044021 (2014).

[17] A. Buonanno, Y. Chen, Y. Pan, and M. Vallisneri, Phys. Rev. D **70**, 104003 (2004).

[18] M. Hannam, P. Schmidt, A. Boh, L. Haegel, S. Husa, F. Ohme, G. Pratten, and M. Prrer, Phys. Rev. Lett. **113**, 151101 (2014).

[19] P. Schmidt, F. Ohme, and M. Hannam, Phys. Rev. D **91**, 024043 (2015).

[20] A. Klein, N. Cornish, and N. Yunes, Phys. Rev. D **88**, 124015 (2013).

[21] K. Chatziioannou, A. Klein, N. Yunes, and N. Cornish, Phys. Rev. D **88**, 063011 (2013).

[22] K. Chatziioannou, N. Cornish, A. Klein, and N. Yunes, Phys. Rev. D **89**, 104023 (2014).

[23] K. Chatziioannou, N. Cornish, A. Klein, and N. Yunes, Astrophys. J. Lett. **798**, L17 (2015).

[24] K. Chatziioannou, K. Yagi, A. Klein, N. Cornish, and N. Yunes, Phys. Rev. D **92**, 104008 (2015).

[25] M. Kesden, D. Gerosa, R. O'Shaughnessy, E. Berti, and U. Sperhake, Phys. Rev. Lett. **114**, 081103 (2015).

[26] A. Klein, N. Cornish, and N. Yunes, Phys. Rev. D **90**, 124029 (2014).

[27] K. G. Arun, A. Buonanno, G. Faye, and E. Ochsner, Phys. Rev. D **79**, 104023 (2009).

[28] D. Shoemaker, Technical Report No. LIGO-T0900288-v3, 2010.

[29] L. Lindblom, B. J. Owen, and D. A. Brown, Phys. Rev. D **78**, 124020 (2008).